Decay of the Slow Calcium Current in Twitch Muscle Fibers of the Frog Is Influenced by Intracellular EGTA

FABIO FRANCINI and ENRICO STEFANI

From the Department of Physiology and Molecular Biophysics, Baylor College of Medicine, Houston, Texas 77030; and the Department of Physiology, Centro de Investigación y Estudios Avanzados del Instituto Politécnico Nacional, México City 07000, México

ABSTRACT The mechanism(s) of the decay of slow calcium current (I_{Ca}) in cut twitch skeletal muscle fibers of the frog were studied in voltage-clamp experiments using the double vaseline-gap technique. I_{Ca} decay followed a single exponential in 10 mM external Ca^{2+} and 20 mM internal EGTA solutions in all pulse protocols tested: single depolarizing pulses (activation protocol), two pulses (inactivation protocol), and during a long pulse preceded by a short prepulse (400 ms) to 80 mV (tail protocol). In single pulses the rate constant of I_{Ca} decay was ~0.75 s^{-1} at 0 mV and became faster with larger depolarizations. I_{Ca} had different amplitudes during the second pulses of the inactivation protocol (0 mV) and of the tail protocol (−20 to 40 mV) and had similar time constants of decay. The time constant of decay did not change significantly at each potential after replacing 10 mM Ca^{2+} with a Ca^{2+}-buffered solution with malate. With 70 mM intracellular EGTA and 10 mM external Ca^{2+} solutions, I_{Ca} also decayed with a single-exponential curve, but it was about four times faster (~3.5 s^{-1} at 0 mV pulse). In these solutions the rate constant showed a direct relationship with I_{Ca} amplitude at different potentials. With 70 mM EGTA, replacing the external 10 mM Ca^{2+} solution with the Ca^{2+}-buffered solution caused the decay of I_{Ca} to become slower and to have the same relationship with membrane potential and I_{Ca} amplitude as in fibers with 20 mM EGTA internal solution. The mechanism of I_{Ca} decay depends on the intracellular EGTA concentration: (*a*) internal EGTA (both 20 and 70 mM) significantly reduces the voltage dependence of the inactivation process and (*b*) 70 mM EGTA dramatically increases the rate of tubular calcium depletion during the flow of I_{Ca}.

INTRODUCTION

In intact fibers of the frog, a transient slow inward Ca^{2+} current (I_{Ca}) that slowly decays during long pulses has been described (Beaty and Stefani, 1976; Stanfield,

Address reprint requests to Dr. Enrico Stefani, Department of Physiology and Molecular Biophysics, Baylor College of Medicine, One Baylor Plaza, Houston, TX 77030.
Dr. F. Francini is on sabbatical leave from the Department of Physiological Sciences, University of Florence, Viale G.B. Morgagni 63, 50134 Florence, Italy.

J. GEN. PHYSIOL. © The Rockefeller University Press · 0022-1295/89/11/0953/17 $2.00 953
Volume 94 November 1989 953–969

1977; Sánchez and Stefani, 1978, 1983; Almers and Palade, 1981; Almers et al., 1981). The decay of I_{Ca} under long maintained depolarizations, could be explained by one or a combination of the following mechanisms: (*a*) voltage-dependent inactivation, i.e., a decline in the Ca channel conductance (Stanfield, 1977; Sánchez and Stefani, 1978, 1983; Fox, 1981; Cota et al., 1983; Cota and Stefani, 1989); (*b*) Ca^{2+} depletion in a restricted extracellular space such as the tubular lumen (Almers et al., 1981; Lorkovic and Rüdel, 1983; Miledi et al., 1983; Arreola et al., 1987) since Ca^{2+} channels are mainly located in the tubular system (Nicola Siri et al. 1980; Almers et., 1981); and (*c*) local internal accumulation of Ca^{2+} in the vicinity of the plasma membrane that reduced the Ca^{2+} driving force and/or induce a Ca^{2+} dependent inactivation process (Brehm and Eckert, 1978; Tillotson 1979; Eckert and Tillotson, 1981; Ashcroft and Stanfield, 1982; Mentrard et al., 1984; Jmari et al., 1986). Interestingly enough, in relation to tubular Ca^{2+} depletion, it appears that a Ca^{2+} pump located in the tubular membrane may help replenish tubular Ca^{2+} content by extruding into the tubular lumen (Scales and Sabaddini, 1979; Bianchi and Narayan, 1982; Hidalgo et al., 1983, 1986; Mickelson et al., 1985).

Previous work from our laboratory performed on intact muscle fibers suggested a voltage-dependent inactivation mechanism for I_{Ca} decay (Sánchez and Stefani, 1978; Cota et al., 1983; Cota and Stefani, 1989). In contrast, in cut muscle fibers with the intracellular medium equilibrated with 80 mM EGTA, I_{Ca} decayed because of Ca^{2+} depletion in the tubular space (Almers et al., 1981). The different results observed in intact muscle fibers with respect to those obtained from cut fibers could be explained by the experimental conditions used: (*a*) extracellular hypertonic solution in intact fibers, and (*b*) high intracellular EGTA (80 mM) in cut fibers.

The aim of the present work is to further analyze the mechanism(s) of I_{Ca} decay in the skeletal muscle of the frog with the cut fiber preparation under different ionic conditions. To this end we used external solutions containing 10 mM Ca^{2+}, or 26 mM free Ca^{2+} buffered with malate and internal solutions with different amounts of the Ca chelator ethyleneglycol-bis-(β-aminoethylether)*N,N,N′,N′*-tetraacetate (EGTA). The main finding we report here is that the mechanism of I_{Ca} decay depends on the intracellular EGTA concentration: (*a*) internal EGTA (both 20 and 70 mM) significantly reduces the voltage dependence of the inactivation process, and (*b*) 70 mM EGTA dramatically increases the rate of tubular calcium depletion during the flow of I_{Ca}.

MATERIALS AND METHODS

Preparation and Voltage Clamp

Electrical recordings were performed in single cut fibers from the semitendinosus muscle of *Rana pipiens* by using the double vaseline-gap technique, similar to the one introduced by Kovács et al. (1983). In these experiments we chose the frog *R. pipiens*, since its inactivation process has a voltage dependence similar to *R. temporaria's*, which is the frog species used by Almers et al. (1981) (Sánchez and Stefani, 1983; Cota et al., 1984). Small radii (*a*) fibers were selected (*a*, 20–30 μm) to reduce tubular-clamp nonuniformities (Sánchez and Stefani, 1983; Cota et al., 1983). In Fig. 1 a schematic diagram of the chamber and the circuit is shown. Vaseline seals, 300 μm wide, divided the exterior of the fiber in three pools; the middle pool

(Fig. 1, *P*) was 300–400 μm wide. The 1–2-cm fiber segment dissected in a relaxing solution was positioned along the chamber, and the fiber ends in the *E* and *I* pools were cut to a length of ~0.5 mm. Pools were separated with vaseline seals that were tightened around the fiber by positioning and pressing a coverslip on top of the fiber. With this procedure, and using soft vaseline, very good seals were obtained. Once the pools were made, the external solution was applied to the middle pool *P*, and the internal solution was applied to the *E* and *I* pools. Electrical measurements started 30–60 min after applying the internal solution. Electrical connections between compartments and circuit elements were made with nonpolarized Ag/AgCl electrodes immersed in a pool containing 3 M KCl. These pools were connected to the compartments via 1 M KCl agar bridges. The membrane of the fiber segment in the middle pool was clamped (Fig. 1). Switches, S_1, S_2, and S_3 were in position *1*. Compartment *E* was held at virtual ground by amplifier A_1, by injecting current to compartment *I*. The circuit was closed to ground via the middle pool, *P*, with amplifier A_4 in the current to voltage converter configuration. The command pulse, referred to ground, was applied to compartment *P* via A_4. Membrane currents were measured via amplifier A_3 as a voltage drop across a 100-kΩ resistance (*R*). The membrane potential referred to ground was monitored via amplifier A_2 between electrodes *E* and *I*. In A_4, the positive input was connected to ground via a pulse generator, the negative input and the output were separately connected to pool *P* (electrodes

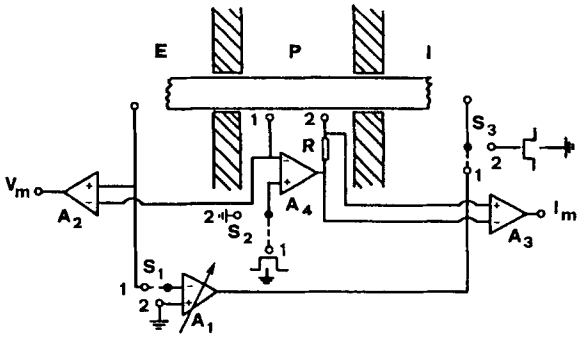

FIGURE 1. Schematic diagram of the chamber and the circuit for the double vaseline-gap technique. The fiber segment in the middle pool was clamped with switches, S_1, S_2, and S_3 in position *1*.

1 and *2*). In this way, possible polarization was avoided at the voltage-recording electrodes *E* and *I*. The membrane potential was sensed at the negative input of the feedback amplifier A_1 and could be attenuated by the finite value of the seal resistance between *E* and *P*. This could introduce a systematic error, constant for each fiber, in the value of the membrane potential during the command pulse. To evaluate this error during a pulse, the membrane potential across the seal and across the membrane via an intracellular glass microelectrode were compared. The error was <3% and was not corrected.

Solutions

The composition of the relaxing solution was (in millimolar): 120 K-glutamate, 1 $MgCl_2$, 5K-Tris-maleate, and 1 Na_2EGTA. The composition of the external and internal solutions are shown in Table I. The external solutions were Cl^-, K^+, and Na^+ free, and had Ca^{2+} as the main permeant ion. The internal solutions were K^+ free and contained TEA^+ or Cs^+, and either 20 or 70 mM-EGTA. The addition of pyruvate, ATP, and glucose to the intracellular solutions increased the time of viability of the preparation (60–120 min) and allowed us to detect both fast and slow I_{Ca} (Cota and Stefani, 1986; García and Stefani, 1987). All solutions were buffered at pH 7.00 ± 0.05.

TABLE I

Composition of Solutions

External solutions						
Solution	$Ca(CH_3SO_3)_2$	$TEA\text{-}CH_3SO_3$	3,4 DAP	TEA-HEPES	$(TEA)_2$-malate	Ca-malate
10 mM Ca^{2+}	10	105	1	5	—	—
Ca^{2+}-buffered	—	—	—	10	15	126

Internal solutions										
Solution	$(TEA)_2$-EGTA	Na-HEPES	NaF	Cs_2-EGTA	$MgCl_2$	Cs-glutamate	Na-pyruvate	Cs-HEPES	Na_2-ATP	Glucose
20 mM EGTA	—	—	20	20	6.9	50	10	10	5	5
70 mM EGTA	70	10	—	—	—	—	10	—	5	5

The Ca^{2+}-buffered solution had 26 mM free Ca^{2+}, assuming a K_d for Ca-malate of 11 mM (Martell and Smith, 1982). All values are in millimolar.

Temperature

The bath temperature was 17°C and was controlled (±0.2°C) by a Peltier system and a thermistor. The temperature was recorded with a probe located ~1 mm from the middle portion of the fiber.

Stimulation, Recording, and Data Analysis

For data acquisition, stimulation, and analysis an IBM AT personal computer was used. Digital-to-analog and analog-to-digital conversion, 12 bits, were done by a Labmaster Interface (Scientific Solutions Inc., Solon, OH). The passive characteristics of the membrane fibers were obtained by applying a 20-mV, 200-ms depolarizing pulse from the holding potential (HP) at −90 mV. Membrane currents during a voltage pulse *P* were initially corrected by analog subtraction of linear components. The remaining linear components were subtracted digitally using P/4 or P/8 control pulses.

The following stimulating protocols were used: (*a*) Activation protocol, 2–5-s depolarizing pulses from an HP of −90 mV in 10-mV increments (P/4); (*b*) inactivation protocol, 5-s prepulse from HP −100 mV in 10-mV increments followed by a 5-s test pulse to 0 mV, between the prepulse and test pulse the fiber was polarized to the HP for 50 ms (P/4); (*c*) tail protocol, 0.4-s prepulse to 80 mV followed by 5-s pulses from −30 to 40 mV in 10-mV increments, HP −90 mV (P/8). Electrical signals were passed through a four-pole Butterworth low-pass filter (Frequency Devices, Inc., Haverhill, MA) with corner frequency set at half the value of the sampling frequency. Membrane currents are generally expressed per unit external surface ($\mu A/cm^2$). Because calcium channels are mainly located in the tubular membranes, I_{Ca} can be normalized per unit fiber volume (mA/ml) to compare current density in fibers with different diameters. Values are given as mean ± SEM with the number of observations (n). The best single or multiple exponential fit of I_{Ca} decay was evaluated by the coefficient of correlation (r).

RESULTS

Ca^{2+} Current in Fibers with 20 mM EGTA Internal Solution and 10 mM Ca^{2+} External Solution

Fig. 2 shows records of I_{Ca} and fitted curves to the decay phase. The fiber was stimulated with the activation protocol. I_{Ca} is shown at different pulse potentials, indicated by numbers in millivolts. The pulses to −50 and −40 mV (*b* and *c*) showed the low threshold, fast I_{Ca} recently described (Cota and Stefani, 1986; García and Stefani, 1987). The slow I_{Ca} becomes evident at −30 mV (*d*) reaching a maximal amplitude close to 0 mV (*f*). In different fibers, the slow I_{Ca} was detected at −40 ± 6 mV ($n = 8$) and reached a maximum value at 0 ± 6 mV ($n = 8$). The normalized *I-V* relationship for I_{Ca} peak currents is shown in Fig. 3 *A* for the fiber of Fig. 2 (*open squares*). The peak I_{Ca} amplitude at 0 mV ranged from −20 to −82 $\mu A/cm^2$ (−44 ± 8 $\mu A/cm^2$, $n = 8$) and the time to peak ranged from 0.40 to 0.85 s (0.48 ± 0.05 s, $n = 8$).

The slow I_{Ca} decayed with a single exponential time course at all potentials explored ($r = 0.994$ to 0.999; Fig. 2). The time constant, τ_d, of I_{Ca} decay at 0 mV pulse was 1.32 ± 0.14 s ($n = 8$). The rate constant, $1/\tau_d$, of I_{Ca} decay increased slightly between −10 and 20 mV and became much faster between 20 and 40 mV

(Fig. 3 *B*, *open symbols*). The rate of I_{Ca} increased between 0 and 40 mV despite the fact that the amplitude of I_{Ca} became smaller over this potential range due to the decrease in driving force for Ca^{2+} (Fig. 3, *A* and *B*, *open symbols*). All values found are encompassed by those observed on intact fibers bathed with 10 mM Ca^{2+} (Sánchez and Stefani, 1978, 1983; Cota et al., 1983, 1984).

In Fig. 4, I_{Ca} records during the inactivation protocol and the corresponding

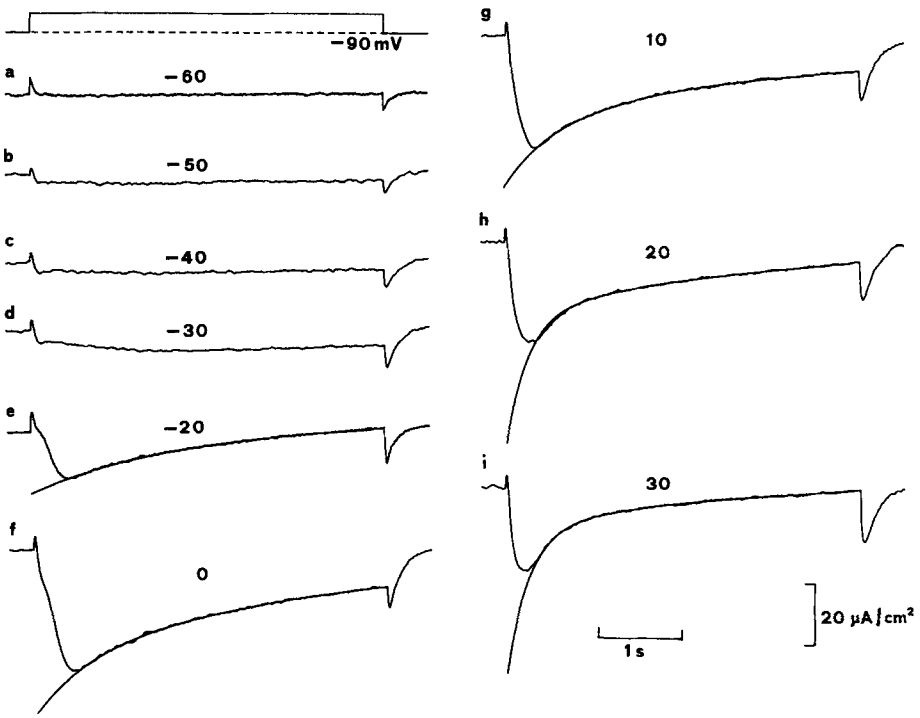

FIGURE 2. Activation protocol with 20 mM EGTA internal and 10 mM Ca^{2+} external solutions. Single depolarizing pulse at different membrane potentials, indicated by the numbers in figures. The fast I_{Ca} is observed in *b* and *c*, −50 and −40 mV pulses, respectively; in *d*, −30 mV pulse, the slow I_{Ca} becomes evident. The I_{Ca} decay in records *e–i* can be fitted with a single exponential curve, r = 0.994–0.998, with the time constant decreasing with increased depolarization. Superimposed computer record of I_{Ca}(*e–i*) and single exponential curve fitted to I_{Ca} decay. Time constants are: 1.61 s (−20 mV), 1.47 s (0 mV), 1.44 s (10 mV), 1.36 s (20 mV), and 1.22 s (30 mV). Temperature, 17°C.

fitted curves are shown. Fig. 5 *A* shows the steady-state inactivation curve (h) for the fiber of Fig. 2 *B* (*open circles*) and for another fiber (*open squares*). The experimental points of the h_∞ curve were fitted to the equation:

$$h_\infty = [1 + \exp(V - V_h)/k_h]^{-1} \quad (1)$$

where V is the membrane potential during the prepulse, V_h the half-inactivation potential (−27.7 ± 2 mV) and k_h a steepness factor (6.2 ± 0.7 mV) (n = 7). Slow I_{Ca}

during the postpulses with different amplitudes decayed with a single exponential with similar time constant values (Figs. 4 and 5 *B*), $\tau_d = 1.37 \pm 0.12$ s ($r = 0.994$ to 0.999; $n = 7$).

In summary, as in the intact fiber (Cota et al., 1983, 1984; Cota and Stefani, 1989) with 20 mM intracellular EGTA, the τ_d was not dependent on I_{Ca} amplitude. However, in intact fibers a steeper relationship was found between membrane potential and rate of I_{Ca} decay (Cota and Stefani, 1989). This indicates that the voltage dependence of the inactivation process is reduced by intracellular EGTA.

In Fig. 6, a 0.4-s prepulse to 80 mV was delivered to fully activate all Ca^{2+} channels. Since the activation curve of I_{Ca} reached its maximum at ~0 mV, the tail current after the 80-mV prepulse that was obtained at postpulse potentials ranging from −10 to 40 mV should reflect amplitude changes because of the modification of the driving force. On the other hand, at more negative potentials, a component

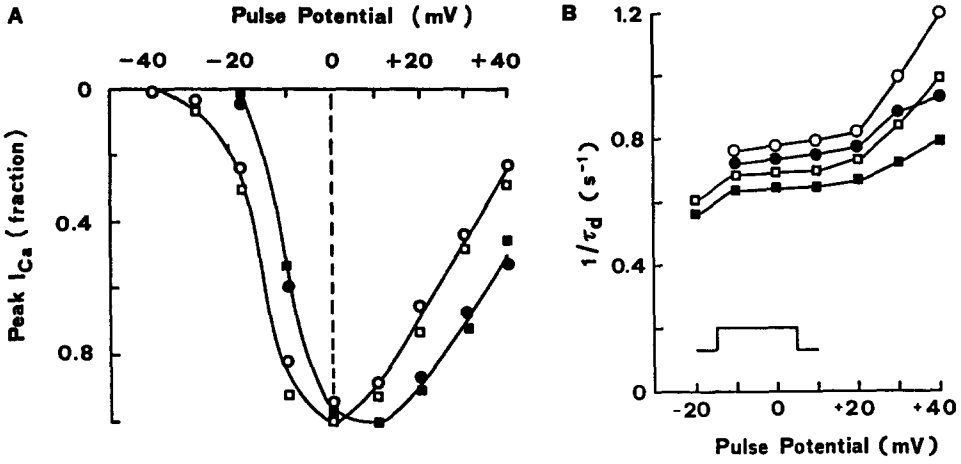

FIGURE 3. Data from two fibers with 20 mM EGTA internal solution and 10 mM Ca^{2+} (*open symbols*) or Ca^{2+}-buffered (*filled symbols*) external solution, at 17°C. (*A*) Normalized *I/V* curves for I_{Ca} peak amplitude. (*B*) Rate constant, $1/\tau_d$, of I_{Ca} decay vs. the membrane potential during the pulse. Open squares and filled circles are from experiments in Figs. 2 and 8 *A*, respectively.

resulting from the deactivation of the Ca^{2+} channels is to be expected. A depletion hypothesis for the decay of I_{Ca} during the pulse, predicts an inverse relationship between I_{Ca} amplitude and the time constant of decay at potentials more positive than 0 mV (Almers et al., 1981). The records show that during the prepulse to 80 mV outward currents predominate. However, upon repolarization, Ca^{2+} inward tail currents are evident. For −30 and −20 mV an initial fast deactivating component was seen. For more positive postpulse potentials, tail currents decayed with a single exponential time course ($r = 0.994$–0.999). The time constant at 0 mV was 1.11 ± 0.09 s (7).

As expected from a reduction of the driving force, the amplitude of I_{Ca} tail, extrapolated to the end of the prepulse, decreased with the pulse potential (Fig. 7 *A*, *open symbols*). Values for pulses to −20 mV ranged from 40 to 110 $\mu A/cm^2$

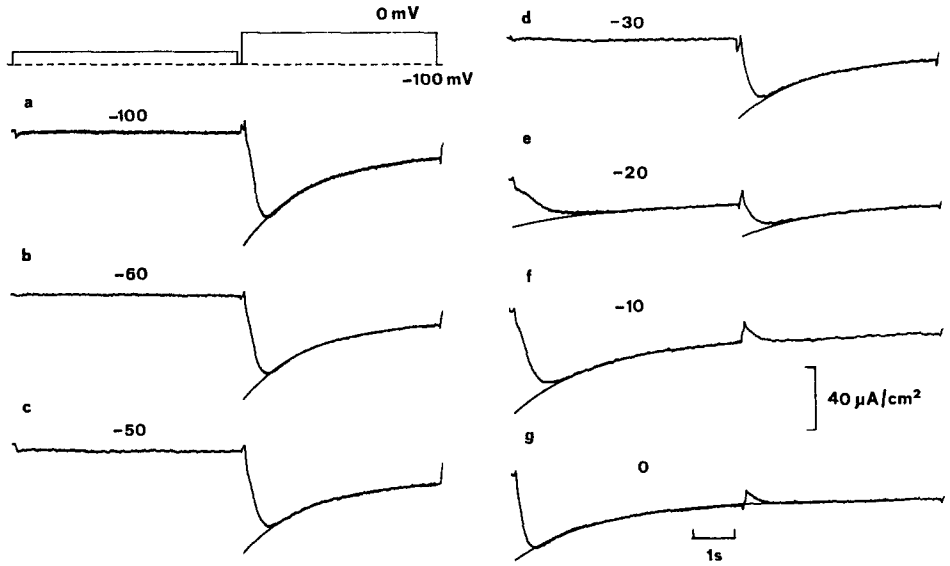

FIGURE 4. Records of I_{Ca} in the same fiber and solutions as in Fig. 2., for inactivation protocol of stimulation at 17°C. Prepulse potential indicated by figures. Records *b* and *c*, −60 and −50 mV prepulse, respectively, show an inactivated I_{Ca} peak during pulse at 0 mV while no slow I_{Ca} is observed during the prepulse. In all records the I_{Ca} decay could be fitted with a single exponential curve, $r = 0.993$–0.999, with a similar time constant: 1.48 s (−100 mV), 1.40 s (−60 mV), 1.49 s (−50 mV), 1.44 s (−30 mV), and 1.43 s (−20 mV). In contrast, during the pulse the time constant of I_{Ca} decays progressively faster with pulse potenial: 1.68 s (−20 mV), 1.54 s (−10 mV), and 1.47 s (0 mV). Superimposed computer record of I_{Ca}, during prepulse and/or pulse and single exponential curve fitted to I_{Ca} decay are shown.

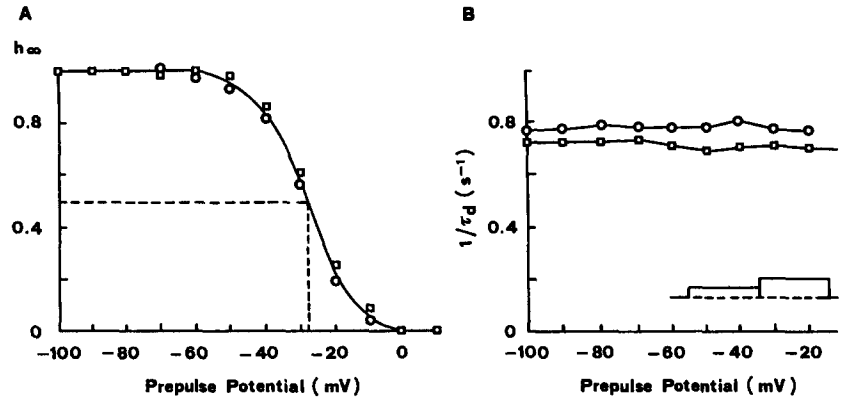

FIGURE 5. Two muscle fibers with 20 mM EGTA internal and 10 mM Ca^{2+} external solution at 17°C. Inactivation protocol of stimulation. (*A*) Normalized I_{Ca} peak amplitude during pulse (h_∞) as a function of the membrane potential during prepulse. Sigmoidal curve corresponds to the best nonlinear fit of the experimental points to Eq. 1. The dashed lines indicate the midpoint of the inactivation curve, $V_h = 27.5$ mV. The steepness of the h_∞ curve is $k_h = 6.3$ mV. (*B*) Rate constant, $1/\tau_d$, of I_{Ca} decay during pulse at 0 mV plotted vs. the membrane potential during the prepulse. Open squares are from the experiment in Fig. 4.

(60 ± 10 $\mu A/cm^2$, $n = 8$). Contrary to the results presented by Almers et al. (1981), the rate constant of decay was practically independent of I_{Ca} amplitude (Fig. 7, *B* and *C*, *open symbols*). It became somewhat faster for large positive potentials. In conclusion, with 20 mM intracellular EGTA it is unlikely that tubular Ca^{2+} depletion is the main cause for the decay of I_{Ca}.

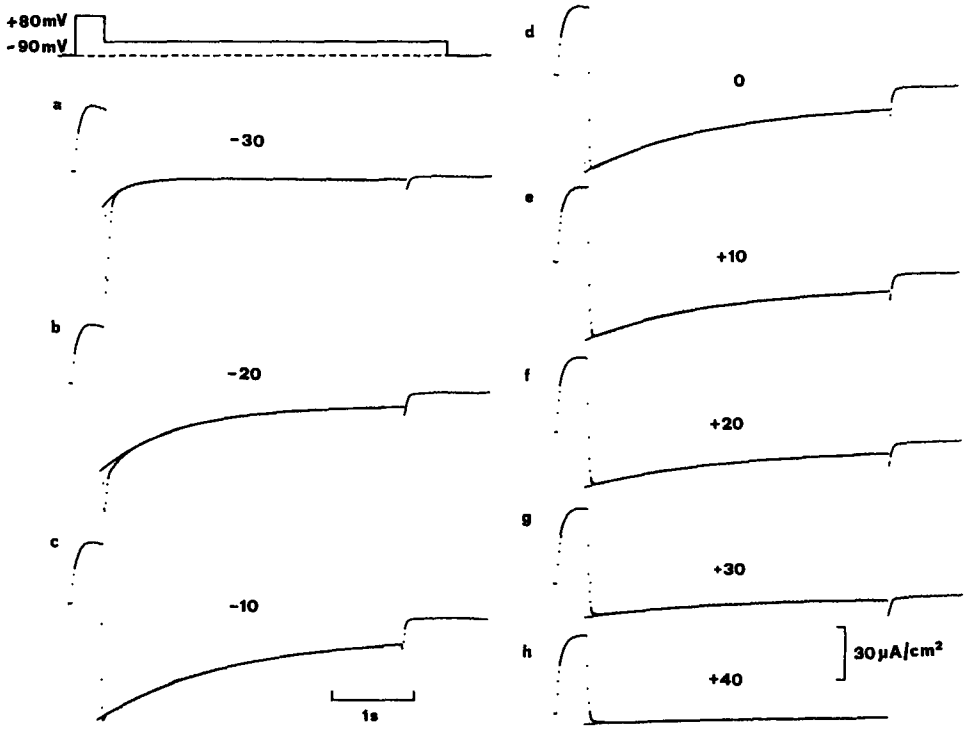

FIGURE 6. Records of I_{Ca} in a fiber with 10 mM Ca^{2+} external soluiton and 20 mM EGTA internal solution to tail protocol of stimulation at 17°C. Pulse potential indicated by figures. At pulse potential more negative than −10 mV not all Ca^{2+} channels are opened, since the maximum I_{Ca} peak to activation protocol of stimulation is at 0 mV, and a fast component on I_{Ca} tail decay is observed. To pulse more positive than −10 mV only a slow component is detected. Superimposed computer records of I_{Ca} tail decay and single exponential curve fitted to the slow component are shown. The time constants are: 0.25 s (−30 mV), 1.05 s (−20 mV), 1.21 s (−10 mV), 1.20 s (0 mV), 1.22 s (10 mV), 1.22 s (20 mV), and 1.06 s (30 mV).

Ca^{2+} Current in Fibers with 20 mM EGTA Internal Solution and Ca^{2+}-buffered External Solution

To further test the depletion hypothesis we used a Ca^{2+}-buffered solution (Almers et al., 1981; Cota and Stefani, 1989). Fig. 8 shows I_{Ca} recordings with the Ca^{2+}-buffered solution. In *A*, I_{Ca} is shown at different pulse potentials; the low threshold fast I_{Ca} is detected at −40 mV (*b*). Larger depolarizations show the slow I_{Ca} with similar characteristics as in Fig. 2 *A*. These observations indicate that I_{Ca} decay cannot be explained by depletion since it was not modified significantly when the exter-

nal Ca^{2+} concentration was buffered (compare in Fig. 3 *B*, *open symbols* with 10 mM Ca^{2+} recording solution and *filled symbols* with Ca^{2+}-buffered solution).

This conclusion was strengthened by tail current experiments. In Fig. 8 *B*, tail currents after a prepulse to 80 mV are shown. Tail amplitudes decrease with pulse potential and in all cases the decay could be well fitted with a single exponential ($r = 0.996$ to -0.999). Furthermore, as in 10 mM Ca^{2+}-recording solution, the decay was practically independent of I_{Ca} amplitude and voltage (Fig. 7, *A*, *B*, and *C*, *filled symbols*).

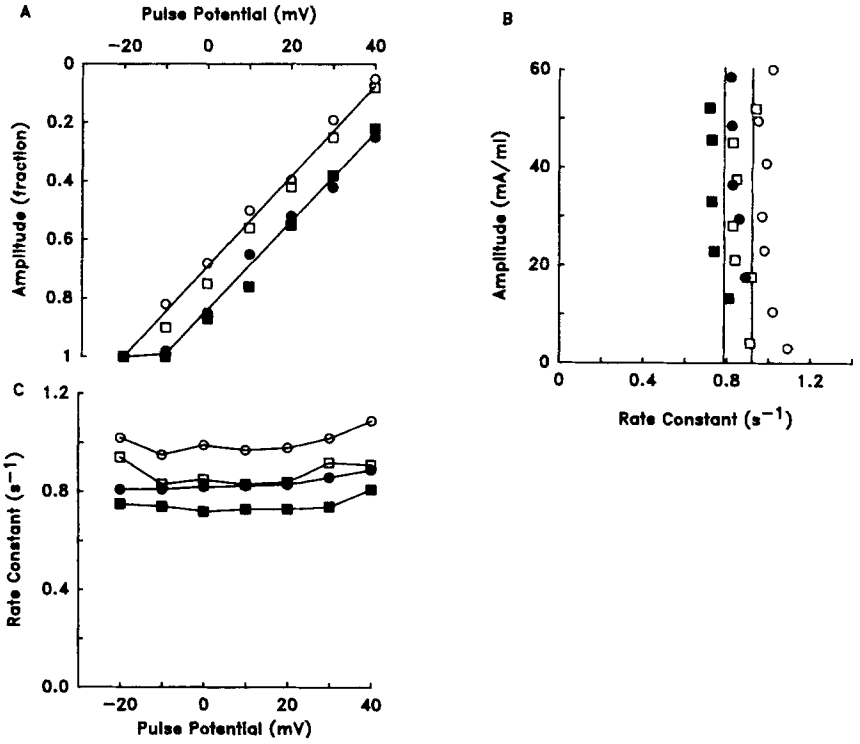

FIGURE 7. Data from two fibers with 20 mM EGTA internal solution and either 10 mM Ca^{2+} (*open symbols*) or Ca^{2+}-buffered (*filled symbols*) external solution at 17°C. Tail protocol of stimulation. Relations between exponential amplitude of I_{Ca} tail decay, extrapolated to time zero (the end of the prepulse) and pulse potential (*A*) or rate constant (*B*). In *C* the rate constant values of I_{Ca} tail decay as a function of the membrane potential during the pulse are shown. Amplitude and rate constant determined by fitting the I_{Ca} tail decay with a single exponential, $r = 0.997$–0.999. Open and filled squares from experiments in Figs. 6 and 8, respectively.

The following differences were found between Ca^{2+}-buffered and 10 mM Ca^{2+} external solution: (*a*) τ_d is somewhat slower, for example at 0 mV 0.76 ± 0.03 s^{-1} (8) and 0.70 ± 0.02 s^{-1} (5), respectively, (see Figs. 3 *B* and 7 *B*); (*b*) I_{Ca} peak amplitude is about two times larger; (*c*) the *I/V* curves for peak I_{Ca} and I_{Ca} tail amplitudes were shifted by $\sim +10$ mV (Figs. 2 *A* and 7 *A*, *filled* and *open symbols*). The 10-mV positive shift and the greater peak I_{Ca} amplitude in the Ca^{2+}-buffered solution is consistent

with a larger ionized Ca^{2+} concentration. The calculated value was 26 mM free Ca^{2+} assuming a K_d for Ca-malate of 11 mM (Martell and Smith, 1982).

Ca^{2+} Current in Fibers with 70 mM EGTA Internal Solution and 10 mM Ca^{2+} External Solution

To test for a possible role of intracellular EGTA in I_{Ca} decay we increased the intracellular EGTA concentration to 70 mM (Almers et al., 1981). The membrane capacity and the decay of the capacity transient during 10-mV pulses from −90 mV were unaffected by high EGTA, indicating the integrity of the tubular network. Capacity

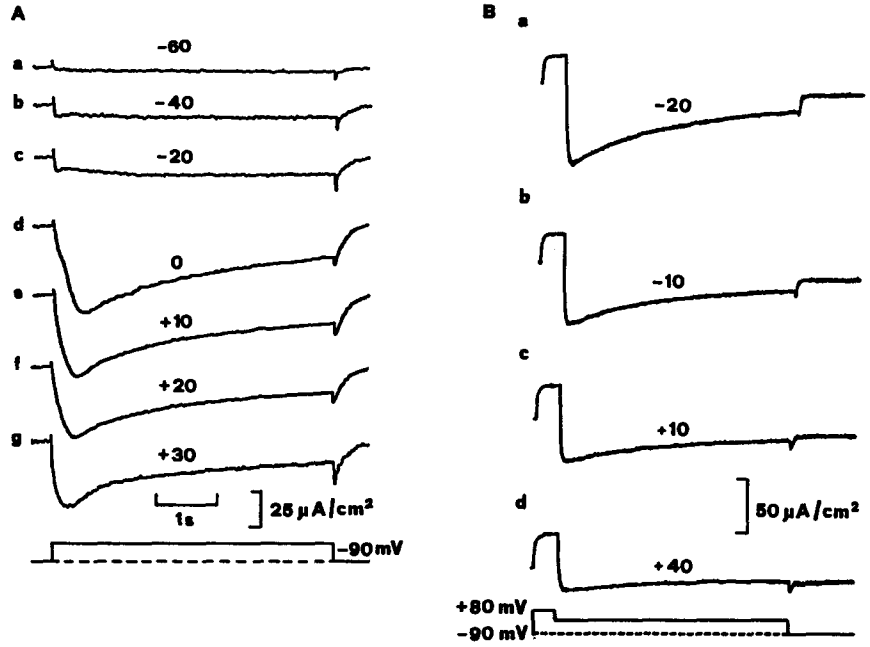

FIGURE 8. Records of I_{Ca} with activation (*A*) and tail (*B*) protocol of stimulation in a fiber with 20 mM EGTA internal solution and Ca^{2+}-buffered external solution. In all records I_{Ca} decay could be fitted with a single exponential curve. Time constant values: (*A*) 1.36 s (0 mV), 1.34 s (10 mV), 1.30 s (20 mV), and 1.24 s (30 mV); (*B*) 1.25 s (−20 mV), 1.26 s (−10 mV), 1.25 s (10 mV), and 1.12 s (40 mV).

values were 9.1 ± 1.5 $\mu F/cm^2$ (12) and 8.9 ± 1.0 $\mu F/cm^2$ (16) in 20 and 70 mM EGTA, respectively. Fig. 9 shows tail current records (*A*) with the superimposed fitted curves (*B*). The decay became slower by increasing the postpulse potential from −30 to 30 mV. For example, τ_d was 0.18 ± 0.015 s (7) at −20 mV and 0.83 ± 0.025 s (7) at 20 mV. These values are significantly faster than those observed in fibers with 20 mM EGTA (1.01 ± 0.02 s [8] at −20 mV and 1.20 ± 0.03 s [8]).

The amplitude of I_{Ca} extrapolated to the end of the prepulse was 51 ± 9 $\mu A/cm^2$ (n = 7). The amplitude decreased with the membrane potential as observed with 20 mM EGTA internal solution (Fig. 10 *A*, *open symbols*). The rate constant, $1/\tau_d$, shows an inverse relation with pulse potential and a direct one with the amplitude. These

results are similar to those described by Almers et al. (1981), indicating that a depletion mechanism was determining the I_{Ca} decay.

Ca^{2+} Current in Fibers with 70 mM EGTA Internal Solution and Ca^{2+}-buffered External Solution

In the previous section we observed that the increase of EGTA concentration in the internal solution made τ_d dependent on the amplitude of I_{Ca}. In this case, if the

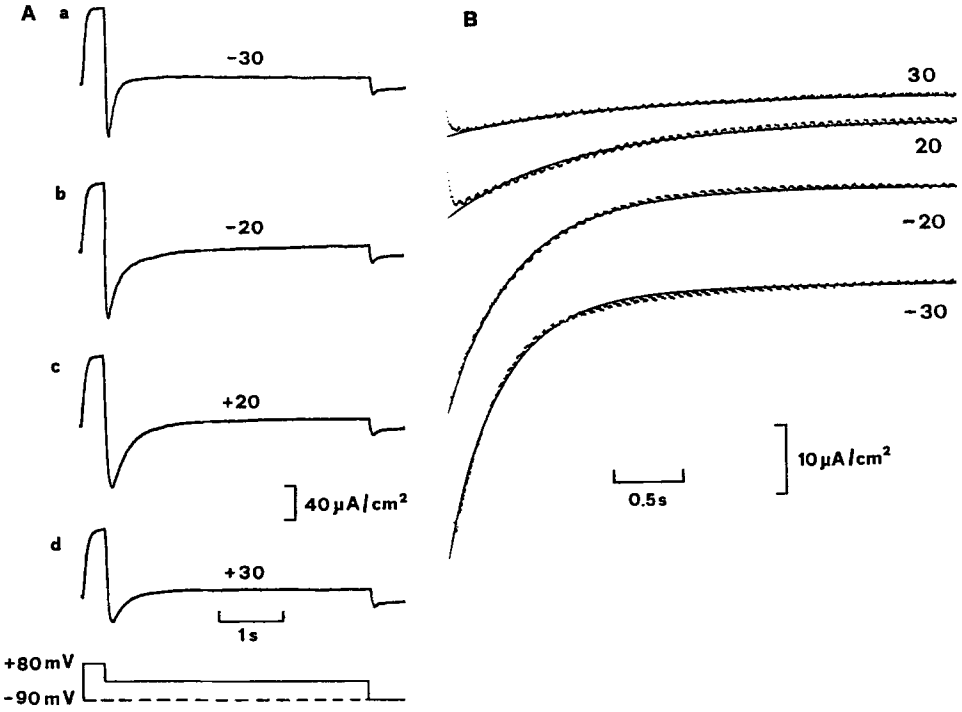

FIGURE 9. Tail pulse protocol of stimulation in a fiber with 70 mM EGTA internal solution and 10 mM Ca^{2+} external solution. In *A*, records of I_{Ca} tail show a progressively slower decay on increasing the pulse potential from *a* to *d*. In *B*, superimposed computer records of I_{Ca} tail shown in *A*, and fitted single exponential curve. The noisier traces are I_{Ca} records. The time constant values are: 0.14 s (−30 mV), 0.19 s (−20 mV), 0.89 s (20 mV), and 1.64 s (30 mV).

decay was due to depletion, buffering the extracellular Ca^{2+} concentration should prevent the decay of I_{Ca}.

Fig. 11 shows records of I_{Ca} decay during tail currents in the same fiber as in Fig. 9, after replacing the 10 mM Ca^{2+} with Ca^{2+}-buffered external solution. The decay was still present, but slower and, as before, it followed a single exponential time course (Fig 11, *A* and *B*). The rate of decay was independent of both I_{Ca} tail amplitude and pulse potential (Figs. 10, *B* and *C*, *filled symbols*, and Fig. 11 *B*). Furthermore, with 70 mM EGTA τ_d was slower than with 20 mM EGTA at all potentials (−10 to 40 mV). For example at 0 mV τ_d values were 1.75 ± 0.16 s ($n = 5$) and

1.37 ± 0.08 (n = 5), respectively. Fig. 10 *A* (*filled symbols*) shows the I/V curve for I_{Ca} amplitude extrapolated at the end of the prepulse. By comparing this curve with that for fibers bathed with 10 mM Ca^{2+}, a positive shift of 10–20 mV to a more positive membrane potential is evident. The tail amplitude for pulse at −20 mV ranged from 40 to 110 $\mu A/cm^2$ (80 ± 17 $\mu A/cm^2$, n = 5).

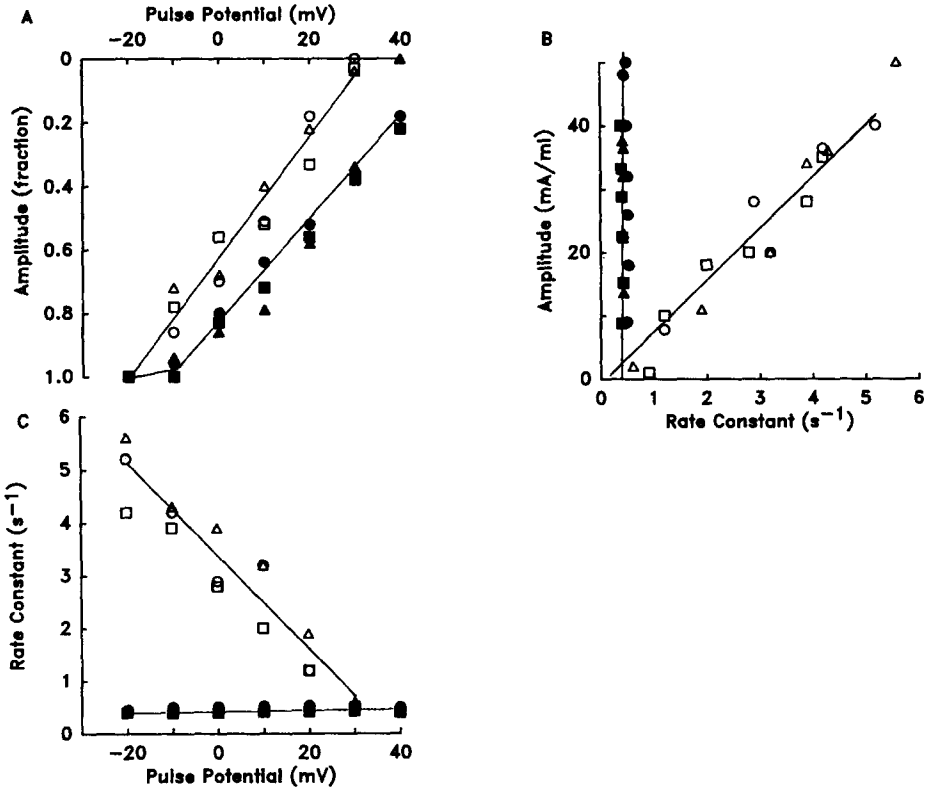

FIGURE 10. Tail protocol of stimulation. Data from three fibers with 70 m M EGTA internal solution and either 10 mM Ca^{2+} (*open symbols*) or Ca^{2+}-buffered solutions (*filled symbols*). Relationships between the normalized exponential amplitude of I_{Ca} decay, extrapolated to time zero (the end of the prepulse) and membrane potential during the pulse are shown in *A*. *B* illustrates the relationship between amplitude and rate constant of decay, while *C* shows the rate constant and the pulse potential.

DISCUSSION

These experiments demonstrate that I_{Ca} decay in cut fibers could be due to different mechanisms depending on the composition of the internal solution used.

Evidence of a Prevalant I_{Ca} Voltage-dependent Inactivation in Fibers with 20 mM EGTA Internal Solution

Fibers bathed with 20 mM EGTA internal solution showed some similarity I_{Ca} decay, with respect to those observed in intact fibers (Sánchez and Stefani, 1978, 1983;

Stefani et al., 1981; Cota et al., 1983; Cota and Stefani, 1989). These similarities were as follows: (*a*) the decay of I_{Ca} was well fitted to a single exponential with time constant values similar to those observed in intact fibers, (*b*) it was not dependent on I_{Ca} peak amplitude either when elicited by single pulses, or when pulses were preceded by prepulses, and (*c*) the rate constant of I_{Ca} decay remained practically unaltered when the 10 mM Ca^{2+} external solution was replaced by the Ca^{2+}-buffered one (Table II).

None of these results can be explained by either a depletion mechanism or an intracellular Ca^{2+}-dependent inactivation mechanism, in which the τ_d depends on

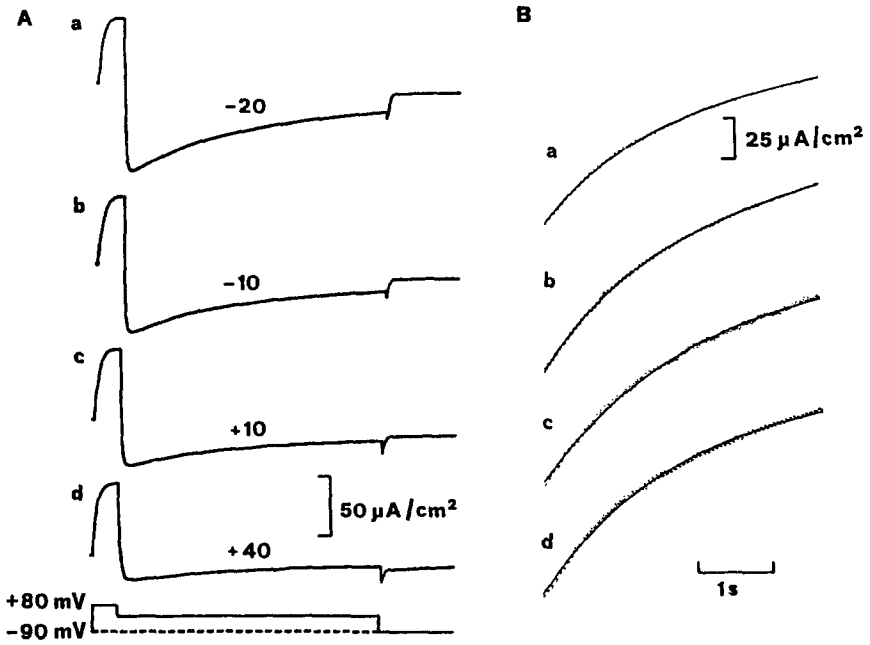

FIGURE 11. Records of I_{Ca} in the same fiber as Fig. 9, after replacing the 10 mM Ca^{2+} external solution with the Ca^{2+}-buffered one for tail protocol of stimulation. In all records I_{Ca} decay follows a single exponential curve, r = 0.996–0.999, and the time constant values are similar to those observed in fibers with 10 mM Ca^{2+} external solution. Records of I_{Ca} in *A* and *B* with a superimposed fitted single exponential curve are shown. In *B* the amplitudes were normalized with respect to the record at −20 mV. The time constants are similar at all pulse potentials (range, 2.1–2.2 s).

Ca^{2+} inward current; thus they are in agreement with a voltage-dependent inactivation process for I_{Ca} decay. Nevertheless, some differences with respect to intact fibers exist. With 20 mM EGTA in the internal solution, the most evident difference is a lesser dependence of the rate constant of I_{Ca} decay on membrane potential (cf. Fig. 3 *B* with Fig. 2 *B* in Cota and Stefani, 1989).

Evidence of a Depletion Mechanism in Fibers with 70 mM EGTA Internal Solution

By increasing the EGTA concentration from 20 to 70 mM, I_{Ca} decay changed dramatically. In two-pulse experiments with a prepulse to 80 mV, the I_{Ca} tail decayed

with a time constant that was about four times faster (Table II). Moreover, the inverse relationship found between $1/\tau_d$ and membrane potential, and the direct one between I_{Ca} tail amplitude and $1/\tau_d$, denote a depletion mechanism. The presence of a depletion mechaniusm was confirmed by the effects of the Ca^{2+}-buffered soltuion on I_{Ca} decay. In fibers bathed with the 70 mM EGTA internal solution, when the 10 mM Ca^{2+} solution was replaced by the Ca^{2+}-buffered one, the I_{Ca} decay could be fitted to a single exponential curve but the decay had a slower time constant, even much slower than in 20 mM EGTA solution. This suggests that 70 mM intracellular EGTA impairs the inactivation mechanism.

Fast I_{Ca} was not recorded either in intact fibers incubated for several hours prior to the experiment, in a solution containing TEA^+ and Cs^+ (Cota et al., 1983), nor was it found in cut fibers bathed with the 80 mM $(TEA)_2$EGTA internal solution (Almers et al., 1981). The presence of glutamate, pyruvate, ATP, and glucose in the internal solution enabled the recording of both fast and slow I_{Ca} and increased the viability of the preparation (García and Stefani, 1987). In the present experiments,

TABLE II

Values of Rate Constant ($1/\tau_d$) of I_{Ca} Decay with a Single Exponential Time Course for Activation and Tail Protocols of Stimulation

Solutions			$1/\tau_d$, in s^{-1}, pulses at 0 *mV*	
External	Internal	*n*	Activation	Tail
10 mM Ca^{2+}	20 mM EGTA	8	0.76 ± 0.03	0.91 ± 0.04
Ca^{2+}-buffered	20 mM EGTA	5	0.70 ± 0.02	0.73 ± 0.02
10 mM Ca^{2+}	70 mM EGTA	7	—	3.51 ± 0.06
Ca^{2+}-buffered	70 mM EGTA	5	—	0.57 ± 0.02

In different bathing solutions I_{Ca} decay followed a single exponential time course. *n* is the number of single fibers. The best fit, with correlation coefficient higher than 0.994, as mean ± SEM, is shown. Temperature, 17°C.

we observed that, with the presence of pyruvate, ATP, and glucose in the internal solution containing 70 mM $(TEA)_2$EGTA, the fast current can be recorded.

In hypertonic external solution, I_{Ca} decay may be explained by a voltage-dependent mechanism (Cota and Stefani, 1989). On the other hand, in isotonic solutions indirect evidence suggests that tubular Ca^{2+} depletion may occur during fiber contracture (Lorkovic and Rüdel, 1983) and in stretched fibers (Miledi et al., 1983). The difference may be explained by the fact that tubular Ca^{2+} depletion may be less significant in fibers bathed with hypertonic solution than in those in an isotonic condition because, in the former, the tubular system has a relatively larger fractional volume (Freygang et al., 1964; Cota et al., 1983). However, in these experiments in isotonic conditions with 20 mM intracellular EGTA, tubular Ca^{2+} depletion was not evident during I_{Ca}. We do not have an explanation for these differences. It may be speculated that the presence of an active transport of Ca^{2+} into the tubular lumen from the myoplasm may reduce Ca^{2+} tubular depletion. This is consistent with the finding that in frog muscle under repetitive stimulation tubular Ca^{2+} concentration is raised by the action of such a Ca^{2+} pump (Bianchi and Narayan, 1982). The reported Ca^{2+} transport into the tubular space was 0.8 $nmol \cdot g^{-1}$ per twitch (wet weight), which corresponds to ~1,350 $pmol \cdot cm^{-2} \cdot s^{-1}$ assuming an action potential duration of 2 ms and a surface membrane area of 300 $cm^2 \cdot g^{-1}$ (wet weight) Bianchi

and Narayan, 1982). From the peak I_{Ca} values at 0 mV (40 $\mu A/cm^2$) the calculated inward Ca^{2+} flow is 200 pmol $cm^{-2} \cdot s^{-1}$, thus the reported pumping rate would be sufficient to sustain the tubular Ca^{2+} concentration during I_{Ca}. On the other hand, biochemical determinations in tubular membrane fractions from mammalian skeletal muscle have demonstrated an ATP-dependent rate of Ca^{2+} uptake of 10 $nmol \cdot mg^{-1} \cdot min^{-1}$ (Hidalgo et al., 1983, 1986; Mickelson et al., 1985) that can be stimulated by calmodulin and cAMP-dependent protein kinase (Mickelson et al., 1985). This Ca^{2+} transport would not be operating in high intracellular EGTA.

In conclusion, Ca^{2+} currents and the decay of the slow I_{Ca} depend on intracellular components. Some of these, such as glutamate, pyruvate, ATP, and glucose, are useful in maintaining the voltage-dependent inactivation process in operation, while EGTA impaired it and made depletion evident. The time constant of I_{Ca} tail decay, probably, represents the upper limits of the depletion mechanism, which operates with 70 mM intracellular EGTA.

The authors are most grateful to Dr. J. García for participating in the initial experiments and for helpful discussion during the work.

This work was supported by National Institutes of Health (RO1 AR-38970).

Original version received 13 December 1988 and accepted version received 26 April 1989.

REFERENCES

Almers, W., R. Fink, and P. T. Palade. 1981. Calcium depletion in frog muscle tubules: the decline of calcium current under maintained depolarization. *Journal of Physiology.* 312:177–207.

Almers, W., and P. T. Palade. 1981. Slow calcium, and potassium currents across frog muscle membrane: measurements with a vaseline-gap technique. *Journal of Physiology* 312:159–176.

Arreola, J., J. Calvo, M. C. García, and J. A. Sánchez. 1987. Modulation of calcium channels of twitch skeletal muscle fibres of the frog by adrenaline, and cyclic adenosine monophosphate. *Journal of Physiology.* 393:307–330.

Ashcroft, F. M., and P. R. Stanfield. 1982. Calcium inactivation in skeletal muscle fibres of the stick insect, *Carausius morosus. Journal of Physiology.* 330:349–372.

Beaty, G. N., and E. Stefani. 1976. Inward calcium current in twitch muscle fibres of the frog. *Journal of Physiology.* 260:27P. (Abstr.)

Bianchi, P. C., and S. Narayan. 1982. Muscle fatigue and the role of transverse tubules. *Science.* 215:295–296.

Brehm, P., and R. Eckert. 1978. Calcium entry leads to inactivation of calcium channels in *Paramecium. Science.* 202:1203–1206.

Cota, G., L. Nicola Siri, and E. Stefani. 1983. Calcium-channel gating in frog skeletal muscle membrane: effects of temperature. *Journal of Physiology.* 338:395–412.

Cota, G., L. Nicola Siri, and E. Stefani. 1984. Calcium channel inactivation in frog (*Rana pipiens* and *Rana montezuma*) skeletal muscle fibres. *Journal of Physiology.* 354:99–108.

Cota, G., and E. Stefani. 1986. A fast-activated inward calcium current in twitch muscle fibres of the frog (*Rana montezume*). *Journal of Physiology.* 370:151–163.

Cota, G., and E. Stefani. 1989. Voltage-dependent inactivation of slow calcium channels in intact twitch muscle fibers of the frog. *Journal of General Physiology.* 94:000–000.

Eckert, R., and D. L. Tillotson. 1981. Calcium-mediated inactivation of the calcium conductance in cesium-loaded giant neurones of *Aplysia californica. Journal of Physiology.* 314:265–280.

Fox, A. P. 1981. Voltage-dependent inactivation of a calcium channel. *Proceedings of the National Academy of Sciences.* 78:953–956.

Freygang, W. H., Jr., D. A. Goldstein, D. C. Hellam, and L. D. Peachey. 1964. The relation between the late after-potential and size of the transverse tubular system of frog muscle. *Journal of General Physiology.* 48:235–263.

García, J., and E. Stefani. 1987. Appropriate conditions to record activation of fast Ca^{2+} channels in frog skeletal muscle (*Rana pipiens*). *Pflügers Archiv.* 408:646–648.

Hidalgo, C., M. E. González, and A. M. García. 1986. Calcium transport in transverse tubules isolated from rabbit skeletal muscle. *Biochimica et Biophysica Acta.* 854:279–286.

Hidalgo, C., M. E. González, and R. Lagos. 1983. Characterization of the Ca^{2+}- or Mg^{2+} -ATPase of transverse tubule membranes isolated from rabbit skeletal muscle. *Journal of Biological Chemistry,* 258:13927-13945

Jmari, K., C. Mironneau, and J. Mironneau. 1986. Inactivation of calcium channel current in rat uterine smooth muscle: evidence for calcium- and voltage-mediated mechansims. *Journal of Physiology.* 380:111–126.

Kovács, L., E. Ríos, and M. F. Schneider. 1983. Measurement and modification of free calcium transients in frog skeletal muscle fibres by a metallochromic indicator dye. *Journal of Physiology.* 343:161–196.

Lorkovic, H., and R. Rüdel. 1983. Influence of divalent cations on potassium contracture duration in frog muscle fibres. *Pflügers Archiv.* 398:114–119.

Martell, A. E., and R. M. Smith. 1982. Critical Stability Constants. Vol. III. Plenum Publishing Corp., New York, London. 124–126.

Mentrard, D., G. Vassort, and R. Fischmeister. 1984. Calcium-mediated inactivation of the calcium conductance in cesium-loaded frog heart cells. *Journal of General Physiology.* 83:105–131.

Mickelson, J. R., T. M. Beaudry, and C. F. Louis. 1985. Regulation of skeletal muscle sarcolemmal ATP-dependent calcium transport by calmodulin and cAMP-dependent protein kinase. *Archives of Biochemistry and Biophysics.* 242:127–136.

Miledi, R., I. Parker, and P. H. Zhu. 1983. Changes in threshold for calcium transients in frog skeletal muscle fibres owing to calcium depletion in the T-tubules. *Journal of Physiology.* 344:233–241.

Nicola Siri, L., J. A. Sánchez, and E. Stefani. 1980. Effect of glycerol treatment on the calcium current of frog skeletal muscle. *Journal of Physiology.* 305:87–96.

Sánchez, J. A., and E. Stefani 1978. Inward calcium current in twitch muscle fibres of the frog. *Journal of Physiology.* 283:197–209.

Sánchez, J. A., and E. Stefani. 1983. Kinetic properties of calcium channels of twitch muscle fibres of the frog. *Journal of Physiology.* 337:1–17.

Scales, D. J., and R. A. Sabaddini. 1979. Microsomal T system: a stereological analysis of purified microsomes derived from normal and dystrophic skeletal muscles. *Journal of Cell Biology.* 83:33–46.

Stanfield, P. R. 1977. A calcium dependent inward current in frog skeletal muscle fibres. *Pflügers Archiv.* 368:267–270.

Tillotson, D. 1979. Inactivation of Ca conductance depends on entry of Ca ions in molluscan neurons. *Proceedings of the National Academy of Sciences.* 76:1497–1500.